METEOROLOGICAL WATER VAPOR RAMAN LIDAR - ADVANCES

T. Dinoev[(1)], **Y. Arshinov**[(3)], **S. Bobrovnikov**[(3)], **I. Serikov**[(2)], **B. Calpini**[(4)], **H. van den Bergh**[(1)] **and V. Simeonov**[(1)]

[(1)] *Air Pollution Laboratory (LPAS), Swiss Federal Institute of Technology (EPFL), CH 1015 Lausanne, Switzerland*
e-mail: valentin.simeonov@epfl.ch

[(2)]*Environmental Fluid Mechanics Laboratory (EFLUM), EPFL, e-mail: ilya.serikov@epfl.ch*

[(3)]*Institute of Atmospheric Optics, Siberian branch of Russian Academy of Sciences, Tomsk, Russia*
e-mail: arshinov@iao.ru

[(4)]*Payerne Aerological Station, MeteoSwiss, Les Invuardes, CH 1530 Payerne, Switzerland*
e-mail: bertrand.calpini@meteoswiss.ch

ABSTRACT

The design and preliminary results from a Raman lidar for day and nighttime measurements of tropospheric water vapor are presented. The system is developed as an eye safe fully automated instrument for meteorological applications (Meteoswiss). A multi-telescope receiver with a "near range" fiber is used having narrow field-of-view and a grating polychromator is used for narrow-band detection.

1. INTRODUCTION

Meteorology relies among others on accurate and frequent high resolution sampling of water vapor in the troposphere. Periodic data assimilation is performed by operational numerical weather forecasting using ground measurements of pressure, temperature, humidity and wind. The vertical profiles of these parameters are provided by routine balloon radiosonde measurements. With typically twice a day radiosonde launches the measurements could prove unrepresentative for fast running meteorological phenomena.

In this paper, we describe the optical design and performance simulations and we present first measurements with a Raman lidar designed for fully-automated day and night-time profiling of the atmospheric water vapor. The system has been developed for the Swiss meteorological service in order to provide additional information on the temporal and spatial variability of the tropospheric water vapor. Supplementary to the humidity radiosonde measurements the data will be used for numerical weather prediction and it is intended to become a source of reference for intercomparison and intercalibration of GPS-based systems.

In order to use the lidar data for weather prediction it is required measurement accuracy better than 10% from 150 m to 5 km during daytime and 150 m to 7.5 km nighttime with between 50 to 300 m vertical resolution and 15 to 30 min temporal resolution. Daytime operation is achieved by implementing narrow band, narrow field of view technique (NB-NFOV) [1]. The use of the NFOV approach leads to high-altitude full overlap that limits the near operational range of the lidar. To extend the lidar operational range to lower altitudes (i.e. 100 m) we derive the water vapor mixing

ratio using regions of incomplete overlap with eliminated range dependence of the lidar calibration constant. The idea of incomplete overlap operation together with a method for aerosol influence correction is presented in part 2. Part 3 describes a NFOV lidar transceiver based on four telescopes coupled by fibers to a diffraction grating polychromator described in part 4, which provides for narrow-band detection. With an additional "near range" fiber in one of the telescopes the near range signal is improved leading to day and night time operation in the required altitude range with a single FOV system. Part 5 presents preliminary day and night time measurements with the system.

2. LIDAR PRINCIPLE

The water vapor mixing ratio $\omega(R)$ is derived from the Q-branch intensities of the ro-vibrational Raman lidar response of atmospheric water vapor $S_{H_2O}(R)$ and nitrogen $S_{N_2}(R)$ [2]:

$$\omega(R) = n \frac{O_{N_2}(R)\eta_{N_2}(R)\sigma_{N_2}}{O_{H_2O}(R)\eta_{H_2O}(R)\sigma_{H_2O}} \frac{S_{H_2O}}{S_{N_2}} \Gamma(R), \qquad (1)$$

where n is a coefficient converting water vapor - nitrogen to water vapor - air mixing ratio, $\Gamma(R)$ is the differential atmospheric transmission at the water vapor and nitrogen wavelengths, σ_X is the Raman cross section of the species x, and $O_X(R)$ and η_X are the overlap functions and the total efficiencies of the respective channels. Since the two Raman signals are excited by a single beam, the ratio of their overlap functions is range independent. Therefore, to use signals with incomplete overlap we have to eliminate the range dependence of η_X, which can be achieved by a suitable receiver-polychromator design. Using incomplete overlap has an additional advantage of reducing the dynamic range of the signals due to geometrical compression.

The differential transmission coefficient $\Gamma(R)$ takes into account the differences in the atmospheric extinction at the water vapor and nitrogen wavelengths and has Raleigh and Mie components. While the Rayleigh component can be calculated from an air density profile, the Mie part is difficult to estimate because of the high temporal and spatial variability of the atmospheric aerosol. Here we propose the use of oxygen Raman backscatter for detection and correction of aerosol

induced errors in water vapor profiles. Using the Angstöm approximation for the aerosol extinction $\alpha_X^a = c\lambda_X^{-p}$, the differential transmission coefficient can be estimated from the ratio of the nitrogen to oxygen signals and a profile of the molecular extinction $\alpha_X^m(R)$:

$$\Gamma(R) = \left(\frac{S_{N_2}}{S_{O_2}} N_{O_2 N_2}\right)^\vartheta e^{\int_{R_0}^{R}\left[\alpha_{H_2O}^m - (1+\vartheta)\alpha_{N_2}^m + \vartheta\alpha_{O_2}^m\right]dr}, \quad (2)$$

where $N_{O_2 N_2}$ is the mixing ratio oxygen - nitrogen and $\vartheta = (\lambda_{H_2O} - \lambda_{N_2})/(\lambda_{N_2} - \lambda_{O_2})$.

An essential design objective is to achieve day-time water vapor measurements to altitudes of up to 5 km. In the case of daytime operation of a Raman lidar, the solar background is the major limitation since its level could be well above the water vapor Raman signal [1, 3]. The daytime background power P_B depends on the *FOV* of the lidar receiver (full angle), its aperture A, the spectral bandwidth $\Delta\lambda$ of the polychromator and the solar spectral radiance I_ν as [4]:

$$P_B = (\pi/4)I_\nu A\, FOV^2 \Delta\lambda \quad (3)$$

The equation is a simplified mathematical expression of the NFOV-NB technique and shows that FOV reduction is more efficient than bandwidth reduction. The minimal FOV however, is limited by the laser beam divergence, the pointing stability and the stability of the lidar alignment. To define the maximal FOV that ensures sufficient measurement accuracy, several configurations of the lidar receiver including multi-telescope (with a different number of mirrors) and single telescope configurations were simulated.
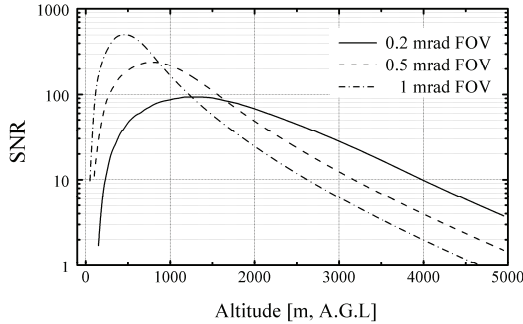

Fig.1. SNR for different FOV of the receiver; configuration with 4 telescopes 30 cm in diameter with f/3.3 and different aperture stops for FOV of 0.2 to 1 mrad

The overlap functions for each configuration were calculated using a model based on the OSLO ray-tracing software (Lambda Research Corporation). The signal-to-noise ratio (SNR) is calculated with 75 m vertical resolution and 15 min averaging time assuming a pure molecular atmosphere, an exponentially decaying water vapor mixing ratio (from 1 g/kg to 0.1 g/kg at 5 km), a polychromator efficiency of 30 % with passband of 0.35 nm (at FWHM), and a solar spectral irradiance of 3.6 $mW/cm^2 sr\mu m$.

The results obtained from calculations with three FOV values using a four telescope configuration described below are shown on Fig.1. It can be seen that a FOV of 0.2 mrad already ensures sufficient SNR for water vapor retrieval for altitudes of up to 5 km. Further reduction of the FOV, however may lead to alignment instability as the divergence of the expanded laser beam is ~ 0.120 mrad. Using spatial averaging from 150 to 300 m will increase the far range SNR.

3. LIDAR TRANSCEIVER

Since the lidar will be used as an automated instrument for routine meteorological observations, it has to have high long-term optical stability and overall reliability. The NFOV-NB technique used to achieve daytime operation of the Raman lidar poses strong requirements to the transmitter beam divergence and pointing stability, as well as to the mechanical and thermal stability of the lidar as a whole. Another important constraint in the lidar design is the eye safety since the lidar will be operated in unattended mode in a populated region with intensive air-traffic.
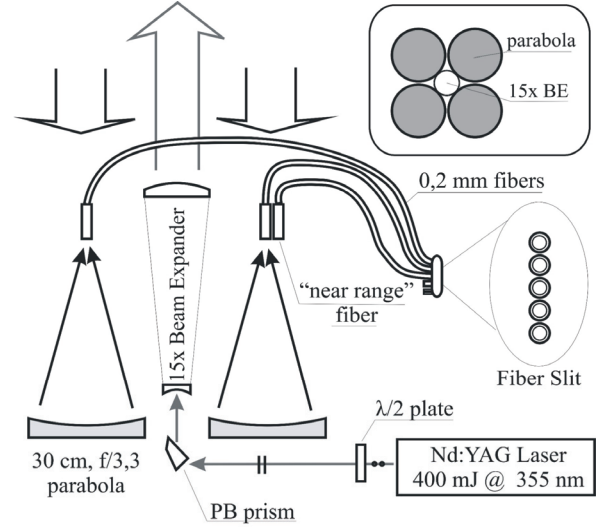

Fig.2. Raman lidar setup

To achieve the required daytime performance the lidar transmitter uses a high pulse-energy laser source. A tripled Nd:YAG laser with 400 mJ energy per pulse, 30 Hz repetition rate and 8 ns pulse duration (Continuum Powerlite 9030) is used. The laser beam is expanded to ~140 mm by a 15 x expander in order to satisfy the eye-safety requirements and to attain the low divergence needed for the NFOV technique. The expander is built with spherical input and aspheric output AR coated fused silica lenses. The laser beam is delivered to the expander by a Brewster angle Pellin-Broca prism (Fig.2). The lidar alignment is performed by tilting the prism instead of using an additional steering mirror after the expander. Thus, the requirements for the stability and precision of the alignment mechanics are reduced by a factor equal to the magnification of the expander (15x in our case).

According to our estimations of the nominal hazard distance (NOHD) the transmitter is eye and skin safe at any distance for exposure times shorter than 5 s (IEC 60825-1), which is sufficient for a vertically operated lidar.

To attain the range independent detection efficiency, needed for incomplete overlap operation, the receiver employs fibers for coupling of the telescope to the lidar polychromator built on diffraction grating. This eliminates the range dependence of the spot size at the input of the polychromator using the fibers as aperture scramblers [5].

A multi-telescope configuration fiber coupled with the spectral unit is employed in the receiver. This configuration has the following advantages over a receiver based on a single telescope with the same surface: compactness leading to a better long-term stability and higher efficiency due to the possibility to use highly reflective dielectric mirror coating and AR coated telescope windows. Furthermore, the mechanical decoupling of the telescope and the spectral unit improves additionally the system reliability.

The receiver consists of four identical, f/3.33, 300 mm in diameter, parabolic mirrors arranged symmetrically around the beam expander with an axial displacement of 235 mm (Fig. 2). The mirrors have dielectric coating with reflectance of 99.9 % for all Raman wavelengths used here. The collected backscattered light is focused on four 0.2 mm core diameter multimode UV-enhanced fibers with NA 0.22, which direct the light to the spectral separation unit (polychromator). In this configuration the FOV of the lidar receiver is 0.2 mrad with full overlap at approximately 3 km.

3.1. Near range coverage

Because of the narrow FOV and operation in non-coaxial configuration, the full overlap is reached at high altitudes (i.e. 3 km). Due to incomplete overlap the near range signal is reduced and do not allow daytime water vapor retrieval with better than 10 % statistical error below 225 m (Fig.1). Hence, we use a new approach to increase the near range signal without widening the FOV of the receiver or using a dual field-of-view.

In this approach an additional "near range" fiber is installed in the focal plane of one of the telescopes, improving the near range collection efficiency. The fiber is displaced at 0.3 mm from the optical axis of the telescope in direction opposite to the beam expander (see Fig.3). A simulated intensity distribution of the backscattered light at the telescope focal plane is shown in Fig. 3. As seen the "near range" fiber collects part of the backscattered light starting from less than 150 m.

Using bigger displacements the fiber will collect light from lower altitudes. Fig. 4 shows modelled lidar signal calculated for two displacements (0.3 mm and 0.7 mm) of the "near range" fiber. The altitude range of the
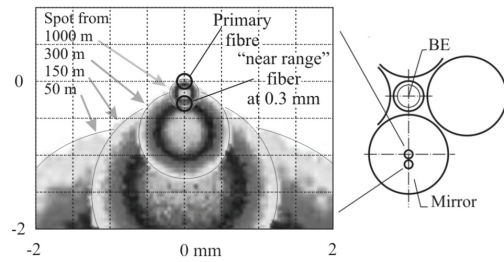

Fig.3. Intensity distribution of the backscatter from different altitudes focused at the focal plane of the 1 m focal length mirror

additional signal is connected to the displacement of the fiber. For the current configuration the fiber (at 0.3 mm) collects light in the range from ~ 100 m to ~ 1500 m while a fiber displaced at 0.7 mm collects in the range from ~ 30 m to ~ 700 m.
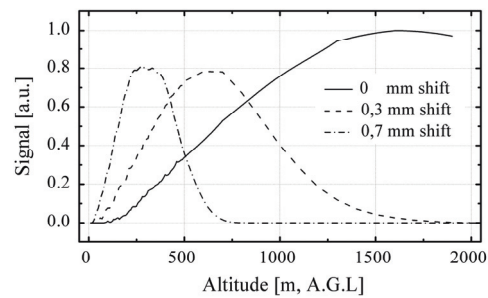

Fig.4. Calculated signal $(A.O(R)/R^2)$ for different displacement of the "near range" fiber (the aberrations of the off-axis usage of the parabola are included using the OSLO)

The SNR for different configurations of the receiver, with or without an additional "near range" fiber, is compared in Fig. 5. The SNR is bigger than 10 from 80 m up to ~ 4 km for 0.2 mm "near range" fiber displaced at 0.3 mm (Conf. 2) when without additional fiber (Conf. 1) this SNR is reached at ~ 225 m. For comparison a configuration with two additional fibers displaced at 0.3 and 0.7 mm having SNR = 50 at 80 m (Conf. 3) and a coaxial telescope (Conf. 4) with the same aperture and 0.2 mrad FOV are presented.
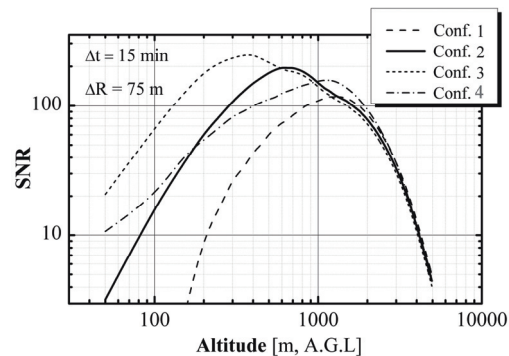

Fig.5. Daytime SNR for water vapor; Configuration 1- four telescopes without "near range" fiber, Conf. 2 - current configuration, Conf. 3 with an additional fiber at 0.7 mm, Conf. 4 - single 600 mm diameter f/3 parabola with FOV 0.2 mrad (0.35 mm field stop)

4. GRATING POLYCHROMATOR

The lidar spectral separation unit is designed to isolate the Q branches of the ro-vibrational Raman spectra of water vapor, nitrogen and oxygen molecules excited by a tripled (354.7 nm) Nd:YAG laser. A diffraction grating polychromator was chosen over to the traditionally used interference filter based polychromators because of the long-term aging effects related to the filters together with possible angular dependence of their transmission, causing problems for incomplete overlap operation.

The polychromator (Fig.6) consists of an input lens collimator (L1-L2), a holographic 3600 gr/mm diffraction grating (85x85 mm^2) with 35.5° incidence angle, and a parabolic mirror. At the input of the collimator is installed a slit formed from five 0.2 mm core diameter fibers connected with the receiver. The calculated pass-band taking into account the aberrations of the polychromator is ~ 0.33 nm at FWHM for the water vapor channel with 1mm output slit.
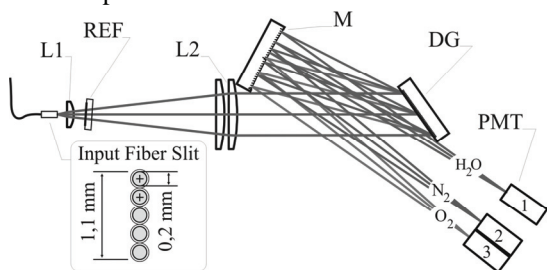

Fig.6. Optical setup of the polychromator; L1-L2 collimator, REF- Raman edge filter, DG - diffraction grating, M – mirror, PMT detectors: (1) water vapor, (2) nitrogen, and (3) oxygen

To maximize the total polychromator throughput we use AR coated lenses and a dielectric coated mirror. However the efficiency is defined mostly by the efficiency of the grating. Measured at water vapor wavelength the total polychromator throughput is 32 %. The cross-talk between the nitrogen and water vapor channels is 3×10^{-8} expected from the low levels of the holographic grating stray light.

The range dependence of the detection efficiency can be associated to range dependent divergence of the light at the output of the fibers used as aperture scramblers [5]. In order to have range independent efficiency, needed for incomplete overlap operation the polychromator is designed to accept without losses the light from NA 0.22 fibers (the divergence measured after fibers coupled to f/3.33 mirror is ~ NA 0.17). With the use of Fourier lens the image of the fiber slit at the output of the polychromator is projected on the PMT surface as a single spot eliminating the PMT spatial detection non-uniformity, causing differences for different fibers.

4. MEASUREMENTS

The lidar has passed the first tests. The absence of range dependence of the calibration constant was proven by measuring the ratio of nitrogen to oxygen signals. The test results have shown also a good correlation between the calculated and the real overlap functions. The first, yet not calibrated, water vapor mixing ratio time series are presented in Fig.7. A vertical water vapor profile from a launched at Payerne meteo-station radiosonde at 24h00 is presented for comparison. Considering the distance between the sites (~ 50 km) the profiles at midnight are comparable.
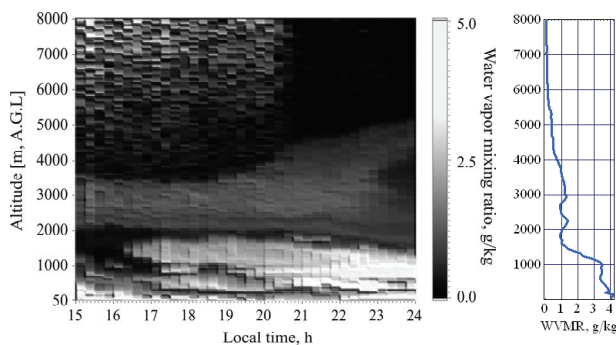

Fig.7. Water vapor mixing ratio measurement on 07.04.2006, from 15h00 till 24h00 CEST (UTC+2h) with range resolution of 75 m and averaging of 15 min. Right - Payerne radiosonde measurement at 24h00 CEST.

5. CONCLUSIONS

A NB-NFOV Raman lidar for operational use in the Swiss meteoservice was designed and built. The lidar transmitter is eye safe based on a tripled Nd:YAG laser. The receiver is built on array of four equal telescopes, fiber coupled to a grating based polychromator. An additional "near range" fiber in one of the telescopes is used to attain the near range coverage eliminating the need of a dual filed of view, thus reducing the complexity of the whole system. Calibration and field tests of the lidar are ongoing. The lidar will be operational at Payerne aerological station from August 2008.

REFFERENCES

1. Bisson S., *et al.*, Narrow-band, narrow-field-of-view Raman lidar with combined day and night capability for tropospheric water-vapor profile measurements, Appl. Opt. **38** (1999), 1841-1849

2. Whiteman D., S. Melfi, R. Ferrare, Raman lidar system for the measurement of water vapor and aerosols in the Earth's atmosphere, Appl. Opt. **31** (1992), 3068-3082

3. Measures, *Laser Remote Sensing, Fundamentals and applications*, New York; Wiley, 1984

4. Marenco F., Brunozzi P.T., Different possibilities for water vapor measurements by lidar in daytime at ENEA's observatory in Lampedusa, Italy: a simulation, J.Opt. A:Pure Appl.Opt. **4** (2002), 408-418.

5. Arshinov Y., *et al.*, Optic-fiber scramblers and a Fourier transform lens as a means to tackle the problem on the overlap factor of lidar, ILRC 22 proceedings, Matera, Italy (2004), 227-230